

**THE GRAND GEOCHEMISTRY OF 4 VESTA: FIRST RESULTS.** T.H. Prettyman,<sup>1</sup> A. Beck,<sup>2</sup> W.C. Feldman,<sup>1</sup> O. Forni,<sup>3</sup> S.P. Joy,<sup>4</sup> D.J. Lawrence,<sup>5</sup> T.J. McCoy,<sup>2</sup> L.A. McFadden,<sup>6</sup> H.Y. McSween,<sup>7</sup> D.W. Mittlefehldt,<sup>8</sup> C.A. Polanskey,<sup>9</sup> M.D. Rayman,<sup>9</sup> C.A. Raymond,<sup>9</sup> R.C. Reedy,<sup>1</sup> C.T. Russell,<sup>4</sup> T.N. Titus,<sup>10</sup> M.J. Toplis,<sup>3</sup> N. Yamashita,<sup>1</sup> <sup>1</sup>Planetary Science Institute (1700 East Fort Lowell, Suite 106, Tucson, AZ 85719-2395, [prettyman@psi.edu](mailto:prettyman@psi.edu)), <sup>2</sup>Smithsonian Institution, <sup>3</sup>University of Toulouse, <sup>4</sup>University of California, Los Angeles, <sup>5</sup>Johns Hopkins University Applied Physics Laboratory, <sup>6</sup>NASA Goddard Space Flight Center, <sup>7</sup>University of Tennessee, <sup>8</sup>NASA Johnson Space Center, <sup>9</sup>JPL, Caltech, Pasadena, CA, <sup>10</sup>USGS Astrogeology Science Center.

**Introduction:** On 12-Dec-2011, the Dawn space-craft commenced low altitude mapping of the giant asteroid, 4 Vesta (264-km mean radius). Dawn's roughly circular, polar, low altitude mapping orbit (LAMO) has a mean radius of 470 km, placing the spacecraft within about 210 km of Vesta's surface. At these altitudes, Dawn's Gamma Ray and Neutron Detector (GRaND) is sensitive to Vesta's elemental composition (Fig. 1). GRaND will acquire data in LAMO for up to 16 weeks, which is sufficient to map the elemental composition of the entire surface of Vesta. The timing of LAMO enables us to report the first results of our geochemistry investigation at this conference. In this abstract, we present an overview of our initial observations, based on data acquired at high altitude and during the first weeks of LAMO.

**GRaND overview.** A detailed description of the GRaND instrument, science objectives and prospective results is given in [1]. At low altitudes, GRaND is sensitive to gamma rays and neutrons produced by cosmogenic nuclear reactions and radioactive decay occurring within the top few decimeters of the surface and on a spatial scale of a few hundred kilometers. From these nuclear emissions, the abundance of several major- and minor-elements, such as Fe, Mg, Si, K, and Th can be determined.

Assuming the howardite, eucrite, and diogenite (HED) meteorites are representative of Vesta's crustal composition [2], then GRaND will be able to map the mixing ratios of whole-rock HED end-members, enabling the determination of the relative proportions of basaltic eucrite, cumulate eucrite, and diogenite as well as the proportions of mafic and plagioclase minerals [1,3]. GRaND will also search for compositions not well-represented in the meteorite collection, such as evolved, K-rich lithologies [4], and outcrops of olivine from Vesta's mantle or igneous intrusions in major impact basins [5]. The search for a possible mesosiderite source region is described in [6]. GRaND will globally map the abundance of H, providing constraints on the delivery of H by solar wind and the infall of carbonaceous chondrite materials.

The chemical data acquired by GRaND will be analyzed within the broader context of the Dawn mission, and will be compared to and integrated with maps of

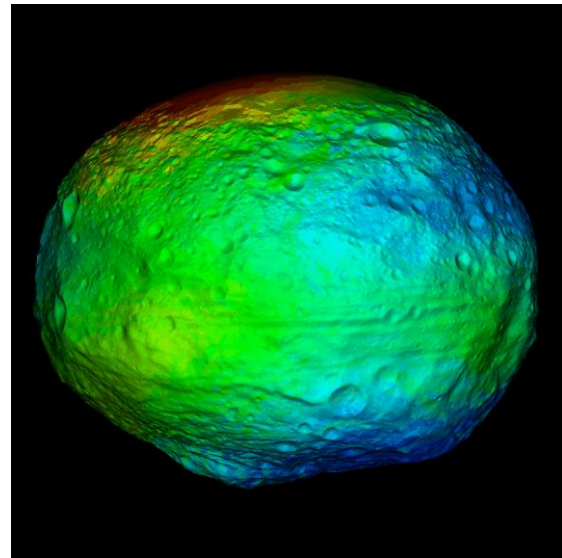


**Figure 1.** Map of counting rates for the  ${}^6\text{Li}(n,{}^3\text{H}){}^4\text{He}$  reaction peak measured by the GRaND's lithium-loaded glass (LIG) scintillator in LAMO. The counting rates have been smoothed by the spatial response of the instrument and superimposed on a shape model for Vesta by R. Gaskell and team [7]. A rainbow color scheme was used (red is maximum). Corrections for solid angle and variations in the flux of galactic cosmic rays have been applied, such that spatial variations can be interpreted as changes in the absorption and moderation of neutrons in Vesta's surface (see **Preliminary Analyses**, second page).

mafic mineral abundances, geologic provinces, gravity, shape and topography. The compositional data acquired by Dawn will provide a more complete picture of Vesta's thermal history and evolution, supplementing geochemical data from HED meteorite studies. GRaND's elemental specificity and depth sensitivity provides a unique view of a compositionally-diverse protoplanet, complementing data acquired by Dawn's Visible-Infrared (VIR) spectrometer and framing camera (FC).

**Initial observations:** Upon approach to high altitude mapping orbit (HAMO) at 950 km mean radius, GRaND detected strong neutron emissions from Vesta. The intensity of neutrons in the thermal, epithermal,

and fast energy ranges increased, varying with the orbital altitude and orientation of the spacecraft, as Dawn descended from HAMO to LAMO. When nadir-pointed, the neutron counting rate is correlated with the solid angle subtended by Vesta at the spacecraft. When corrected for solid angle and variations in the flux of galactic cosmic rays, the neutron output of Vesta in the epithermal energy range is significantly higher than measured by GRaND at Mars. This result supports Vesta having a much lower abundance of hydrogen than Mars. We will compare the neutron spectrum of Mars and Vesta, as measured by GRaND [1], to data acquired by Lunar Prospector and Mars Odyssey at the Moon and Mars [8]. Comparisons of the relative variation of thermal, epithermal, and fast neutrons will show how Vesta's composition differs from the terrestrial planets.

Within about 600-km radial distance, the 7.6-MeV Fe neutron capture gamma ray appeared as a strong peak in the spectrum measured by GRaND's bismuth-germanate (BGO) scintillator. The appearance of the Fe peak was accompanied by increases in other energy ranges, which have contributions from O, Si, and Mg. Th and K have not yet been detected on a global scale, consistent with very low concentrations of these elements in the HED meteorites. Detection limits will be presented in order to provide upper bounds on the abundances of elements not quantified.

**Preliminary analyses:** GRaND has already had sufficient accumulation time and spatial coverage at high altitude and in LAMO to map strong emissions, including thermal and epithermal neutrons, with full global coverage, and to investigate how counting rates for Fe [9] and fast neutrons [10] vary with latitude. Corrections for cosmic ray production and solid angle have been applied, revealing compositional variations on the surface of Vesta. For example, the corrected counting rate for neutron capture with  $^{6}\text{Li}$  in GRaND's lithium-loaded glass (LiG) scintillator, our strongest signature, is shown in Fig. 1.

The LiG counting rate is sensitive to the leakage flux of thermal and epithermal neutrons [1]. Thermal neutrons are sensitive to the abundance of Fe, and other strong neutron absorbers that may be present in Vesta's surface. Epithermal neutrons are sensitive to the abundance of H. The global variation in mapped LiG counting rates is larger than expected for H-free, whole-rock HED compositions, but lower than would be expected, based on modeling, for the whole range of lunar compositions [1]. Consequently, some of the observed variation may be associated with H. Epithermal neutron counting rates measured by a different sensor will be combined with the LiG measurements to separately determine neutron absorption and the abundance of H [1].

It may be possible to determine H-layering by combining information from different neutron energy ranges [1,11, 12].

The north polar region is presently in seasonal darkness, but is visible to GRaND. Neutron counting rates in this region will be monitored for changes as solar illumination increases. A temporal variation in the thermal neutron energy range would provide further information about near-surface thermal properties complementary to that derived from infrared spectroscopy [13,14,15]. Variations in the counting rates in the epithermal and fast energy ranges, although unexpected, could indicate the transport of volatile compounds out of the warming polar region.

**Implications:** The data acquired by GRaND so far indicate that, at a minimum, we will be able to map counting rates for thermal, epithermal, and fast neutrons, and use them to determine the abundance of H and H-layering, neutron absorption, and average atomic mass. We will also analyze the gamma ray spectrum using previously-developed methods [16, 17] to determine the abundance of Fe, Si, and Mg. The abundance of specific elements and constraints will be combined to determine HED end-member mixing ratios. The data acquired by GRaND reinforce the conclusion that Vesta is unusual compared to smaller asteroids, because its surface elemental composition shows considerable variation on a global scale; however, our full interpretation requires additional accumulation time and analysis. By this conference, we will be able to answer many of the science questions posed here and in [1].

**Acknowledgements:** This work was funded by the NASA Dawn mission.

**References:** [1] Prettyman T.H. et al. (2011) *Space Sci. Rev.*, DOI 10.1007/s11214-011-9862-0. [2] Drake M.J. (2001) *Meteorit. Planet. Sci.* 36, 501-513. [3] Usui T. et al. (2010) *Meteorit. Planet. Sci.*, DOI 10.1111/j.1945-5100.2010.01071.x [4] Barrat et al. (2009) *Meteorit. Planet. Sci.* 44:359-374. [5] Beck and McSween (2010) *Meteorit. Planet. Sci.*. DOI 10.1111/j.1945-5100.2010.01061.x [6] Mittlefehldt D.W. et al., submitted to *LPS XLIII*. [7] Raymond, C.A. (2011) *Space Sci. Rev.* DOI:10.1007/s11214-011-9863-z. [8] Feldman, W.C. (2002), *Science*, DOI: 10.1126/science.1073541. [9] Yamashita, N. et al., submitted to *LPS XLIII* [10] Lawrence, D.J. et al., submitted to *LPS XLIII*. [11] Lawrence, D.J. et al. (2011) *JGR*, doi:10.1029/2010JE003678. [12] Feldman, W.C. (2011) *JGR*, doi:10.1029/2011JE003806. [13] Capria, M.T. et al., submitted to *LPS XLIII*. [14] Tosi, F. et al., submitted to *LPS XLIII*. [15] Titus, T.N. et al., submitted to *LPS XLIII*. [16] Lawrence, D.J. et al. (2002) *JGR*, doi:10.1029/2001JE001530. [17] Prettyman, T.H. et al. (2004) *JGR*, doi:10.1029/2003JE002139.